Reduced-Complexity Iterative-Detection-Aided Generalized Space-Time Shift Keying

Shinya Sugiura, *Senior Member, IEEE*, Chao Xu, *Student Member, IEEE*, Soon Xin Ng, *Senior Member, IEEE*, and Lajos Hanzo, *Fellow, IEEE*

***Abstract*—A novel reduced-complexity soft decision (SoD)-aided detector is proposed for the recent concept of space-time shift keying (STSK), where the detector's achievable performance is capable of closely approaching that of the optimal maximum *a posteriori* (MAP) detector. More specifically, we exploit a hybrid combination of the modified matched filtering concept and of reduced-complexity exhaustive search for the sake of reducing the MAP detector's decoding complexity. Furthermore, we extended this detector to support the class of generalized STSK (GSTSK) scheme that subsumes diverse multiple-input–multiple-output (MIMO) arrangements. The proposed reduced-complexity SoD-aided GSTSK detector also attains significantly lower complexity than the MAP detector while imposing only marginal performance degradation, which is in the range of 1–2 dB. As an optional means of further reducing complexity, the Markov Chain Monte Carlo (MCMC) algorithm is invoked for the proposed GSTSK detector. Our EXtrinsic Information Transfer (EXIT) chart analysis reveals that the proposed STSK detector is capable of closely approaching the optimal performance, whereas the GSTSK detector advocated exhibits a modest performance gap with respect to the max-log MAP detector.**

***Index Terms*—EXtrinsic Information Transfer (EXIT) chart, Markov chain Monte Carlo (MCMC), multiple-antenna array, soft decision, space-time shift keying (STSK), turbo coding.**

I. Introduction

THE RECENT universal space-time coding concept of space-time shift keying (STSK) [1], [2] enables us to strike a flexible tradeoff between the maximum achievable diversity gain and the throughput attained. This benefit accrues from the STSK scheme's unique bit-mapping principle, where one out of Q dispersion matrices are activated and detected, which allows us to implicitly signal $\log_2 Q$ additional bits. Moreover, the STSK family includes the space-shift keying (SSK) [3]–[5] and spatial modulation (SM) [6]–[9] schemes as its special cases, where one out of M transmit antenna elements is activated during each symbol interval. Furthermore, in [10], the so-called generalized STSK (GSTSK) scheme was proposed, which is characterized by activating an appropriately configured number of P matrices out of Q dispersion matrices. Owing to its unified architecture, the GSTSK scheme subsumes diverse multiple-input–multiple-output (MIMO) arrangements, such as space-time block coding, the Bell Laboratories' Layered Space-Time (BLAST) scheme, linear dispersion coding [11], STSK, SSK, SM, generalized SSK [12], and the generalized SM [13] schemes. This implies that the GSTSK scheme is capable of striking a flexible diversity, multiplexing, and complexity tradeoff by amalgamating three different encoding principles: 1) dispersion-matrix activation; 2) spatial multiplexing; and 3) amplitude phase modulation.

Diverse hard-decision detectors have been developed for the class of uncoded STSK arrangements,[1] which are free from interelement interference (IEI). The majority of the previously proposed uncoded STSK schemes employed the optimal maximum-likelihood (ML) detection of [1], [3], and [7]. For the sake of approaching the ML detector's performance without substantial performance degradation, the sphere decoding algorithm was applied to the STSK family in [14]. More recently, in [15], the near-optimal matched-filter (MF)-based search algorithm was proposed, which is capable of closely approaching the ML detector's optimal performance while facilitating significant decoding complexity reduction, compared to that of the ML detector. Moreover, since GSTSK relies on three rather diverse encoding schemes and its detection algorithm is substantially different from those of the previous MIMO schemes [16], it is quite a challenging task to develop an efficient and near-optimal detection algorithm. For this reason, its hard-decision algorithm has been limited to the exhaustive ML detector of [10].

Considering that MIMO systems typically rely on powerful channel codes, such as turbo codes [17] and low-density parity-check codes [18], the associated MIMO detector has to provide soft decision (SoD)-based information. However, the SoD-aided STSK detector has not been documented as extensively as its hard-decision counterpart. More specifically, the optimal maximum *a posteriori* (MAP) detector was typically considered for the turbo-coded SSK [3], STSK [1], and

Manuscript received February 29, 2012; revised May 22, 2012; accepted June 21, 2012. Date of publication June 26, 2012; date of current version October 12, 2012. The work of S. Sugiura was supported in part by a Grant-in-Aid for Scientific Research (KAKENHI 23760353) from the Ministry of Education, Culture, Sports, Science, and Technology of Japan. This work was supported in part by the RC–U.K. under the auspices of the India–U.K. Advanced Technology Centre, by the China–U.K. fourth-generation wireless systems project, and by the European Union under the auspices of the Optimix project. The review of this paper was coordinated by Prof. W. A. Hamouda.

S. Sugiura is with Toyota Central R&D Laboratories, Inc., Nagakute 480-1192, Japan (e-mail: sugiura@ieee.org).

C. Xu, S. X. Ng, and L. Hanzo are with the School of Electronics and Computer Science, University of Southampton, SO171BJ Southampton, U.K. (e-mail: lh@ecs.soton.ac.uk).

Color versions of one or more of the figures in this paper are available online at http://ieeexplore.ieee.org.

Digital Object Identifier 10.1109/TVT.2012.2206065

[1] As previously mentioned, since SM and SSK schemes exhibit the same signal structure as that of the STSK scheme, a detection algorithm is interchangeably applicable between these schemes. For this reason, the SM and SSK schemes will be simply referred to as "STSK" in the rest of this paper.

GSTSK schemes [10]. Relying on a novel approach, in [19], a reduced-complexity SoD-based detector was developed for the differentially encoded STSK scheme, where the associated complexity was reduced to 75% of the max-log MAP detector's complexity at the cost of a modest performance degradation.

Against this background, the novel contributions of this paper are given as follows:

1) We propose a reduced-complexity SoD-based detector for the STSK scheme, where we exploit the hybrid combination of the modified MF [15] and of the SoD-based exhaustive search. The proposed detector is capable of attaining lower complexity than the previously developed SoD STSK detector while closely approaching the MAP detector's optimal performance.
2) Another contribution of this paper is that the proposed SoD-based STSK detector was extended to support GSTSK arrangements, hence conceiving the first reduced-complexity GSTSK detector. It is confirmed by our simulations that the performance difference between the proposed detector and the optimal MAP detector is as low as a few decibels for the three-stage-concatenated iteratively detected GSTSK arrangement advocated.
3) As an optional means that is capable of further reducing the proposed GSTSK detector's complexity, we invoke the Markov chain Monte Carlo (MCMC) concept [20]. This allows us to efficiently approximate the action of the SoD-based GSTSK detector without any significant performance loss, noting that the conceived MF and MCMC-based calculations is specifically designed for our GSTSK arrangement.

The remainder of this paper is organized as follows: Section II provides the STSK scheme's system model and the proposed reduced-complexity SoD detector. In Section III, the proposed detector is then modified to support the GSTSK scheme. The related numerical analysis is carried out in Section IV. Finally, our conclusions are presented in Section V.

II. Reduced-Complexity Soft-Decision Space-Time Shift Keying Detector

In this section, we first review the system model of the iteratively detected STSK scheme [1]. Then, we propose the aforementioned reduced-complexity SoD STSK detector.

A. System Model of the STSK Scheme

In this paper, we invoke the three-stage-concatenated turbo principle [21], [22] for the STSK scheme for the sake of achieving near-capacity performance. Fig. 1 shows the schematic of the three-stage channel- and unity rate-coded (URC) STSK scheme using iterative detection. Here, the input source bits are channel encoded by a half-rate recursive systematic convolutional (RSC) code, and they are interleaved by a random bit interleaver Π_1. Then, the interleaved bits are further encoded by a recursive URC encoder [23],[2] and then, the coded bits

[2]The role of the URC is to impose an infinite impulse response, which improves the achievable iterative decoding performance by efficiently spreading the extrinsic information, as detailed in [21].

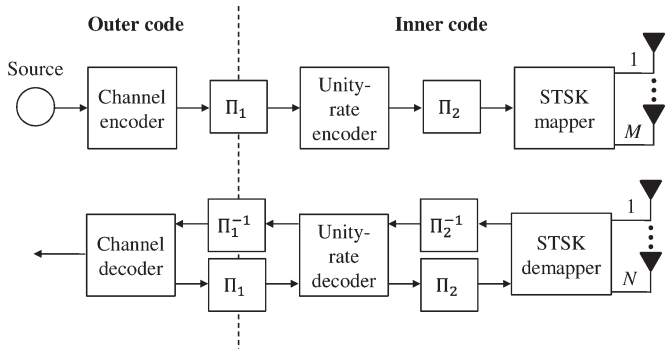

Fig. 1. Schematic of a three-stage RSC- and URC-coded STSK scheme using iterative detection.

are interleaved by the second random interleaver Π_2 of Fig. 1. Finally, the interleaved bits are input to the STSK-mapping block, followed by the transmission of the STSK signaling block.

As shown in Fig. 1, a three-stage iterative decoding algorithm is employed at the receiver. To be specific, the three SoD decoders of the receiver iteratively exchange soft extrinsic information in the form of log likelihood ratios (LLRs). The STSK demapper block of Fig. 1 receives its input signals from the MIMO channels, which are combined with the extrinsic information provided by the URC decoder. Simultaneously, the URC decoder block of Fig. 1 receives extrinsic information from both the RSC channel decoder and the STSK demapper and generates extrinsic information for both of its surrounding blocks seen in Fig. 1. The RSC channel decoder of Fig. 1 exchanges extrinsic information with the URC decoder and outputs the estimated bits after the $I_{\rm out}$ iterations. Here, the iterations between the STSK and URC decoder blocks are referred to as inner iterations, whereas those between the URC and RSC decoders are referred to as outer iterations. The corresponding number of iterations is denoted by $I_{\rm in}$ and $I_{\rm out}$, respectively. Note that $I_{\rm in}$ inner iterations are implemented per outer iteration, indicating that the total number of iterations becomes $I_{\rm in} \cdot I_{\rm out}$.

Let us now consider the STSK-mapping block [1] having M antenna elements, where Q space-time dispersion matrices of $\mathbf{A}_q$ $(q = 1, \ldots, Q) \in \mathcal{C}^{M \times T}$ are designed prior to transmissions, noting that T represents the number of symbol durations per space-time block. Here, $\mathcal{C}^{\xi \times \zeta}$ denotes a complex-valued matrix, having the size of $(\xi \times \zeta)$. More specifically, $B = \log_2 Q + \log_2 \mathcal{L}$ URC-encoded bits, which are input to the STSK encoder during each block interval, are serial-to-parallel (S/P) converted to $B_1 = \log_2 Q$ bits and $B_2 = \log_2 \mathcal{L}$ bits. According to the B_1 bits, one out of the Q dispersion matrices $\mathbf{A}_q$ is activated, whereas B_2 bits are mapped to an $\mathcal{L}$-PSK/QAM symbol s_l. Then, the STSK codeword is generated as follows:

$$\mathbf{S}_{q,l} = s_l \mathbf{A}_q \tag{1}$$

assuming that a dispersion-matrix set is constrained by the following relationship: $\mathrm{tr}[\mathbf{A}_q \mathbf{A}_q^H] = T$ $(q = 1, \ldots, Q)$ to have unity power per symbol duration.

At the N-antenna STSK receiver, the received signals $\mathbf{Y} \in \mathcal{C}^{N\times T}$ may be expressed as

$$\mathbf{Y} = \mathbf{H}\mathbf{S}_{q,l} + \mathbf{V} \tag{2}$$

where the elements of the channel matrix $\mathbf{H} \in \mathcal{C}^{N\times M}$ are the random variables obeying the complex-valued Gaussian distribution of $\mathcal{CN}(0,1)$, whereas $\mathbf{V} \in \mathcal{C}^{N\times T}$ represents the additive white Gaussian noise, which obeys the distribution of $\mathcal{CN}(0, N_0)$. Furthermore, N_0 represents the noise variance, and $\mathcal{CN}(\alpha,\beta)$ denotes a complex-valued Gaussian distribution with a mean of α and a variance β. To arrive at the equivalent system model expressed in vectorial form, the stacking operation is carried out on both sides of (2). Then, we arrive at [1]

$$\bar{\mathbf{Y}} = \bar{\mathbf{H}}\mathbf{K}_{q,l} + \bar{\mathbf{V}} \tag{3}$$

where we have $\bar{\mathbf{Y}} = vec(\mathbf{Y}) \in \mathcal{C}^{NT\times 1}$, $\bar{\mathbf{V}} = vec(\mathbf{V}) \in \mathcal{C}^{NT\times 1}$, $\bar{\mathbf{H}} = (\mathbf{I}_T \otimes \mathbf{H})\chi \in \mathcal{C}^{NT\times Q}$, $\chi = [vec(\mathbf{A}_1), \ldots, vec(\mathbf{A}_Q)] \in \mathcal{C}^{MT\times Q}$, and

$$\mathbf{K}_{q,l} = [0,\ldots,0,s_l,0,\ldots,0]^T \in \mathcal{C}^{Q\times 1}. \underset{\text{the } q\text{th position}}{\uparrow} \tag{4}$$

Here, $\otimes$ represents the Kronecker product, and $vec()$ denotes the vectorial stacking operation [1]. We note from (3) and (4) that STSK does not suffer from any IEI effects, unlike the classic spatial-multiplexing-assisted MIMO systems. The signal vector of (4) contains only a single nonzero element in the qth position of $\mathbf{K}_{q,l}$.

B. Proposed SoD STSK Detector

In this section, we introduce the proposed reduced-complexity SoD STSK detector, which outputs extrinsic information $L_{\mathrm{e}}(b_i)$ $(i = 1,\ldots,B)$ in the form of LLRs based on the input information, i.e., the received signals $\mathbf{Y}$, the channel coefficients $\mathbf{H}$, the noise variance N_0, and the *a priori* LLR $L_{\mathrm{apr}}(b_i)$.

First, the channel coefficients $\mathbf{H}$ are transformed to the equivalent channel matrix $\bar{\mathbf{H}}$ according to the aforementioned relationship of $\bar{\mathbf{H}} = (\mathbf{I}_T \otimes \mathbf{H})\chi$. Then, each column of $\bar{\mathbf{H}}$ is normalized as follows [15]:

$$\acute{\mathbf{H}} = \left[\frac{\bar{\mathbf{h}}_1}{\|\bar{\mathbf{h}}_1\|}, \ldots, \frac{\bar{\mathbf{h}}_Q}{\|\bar{\mathbf{h}}_Q\|}\right] \tag{5}$$

where $\bar{\mathbf{h}}_q$ denotes the qth column of $\bar{\mathbf{H}}$. Then, we invoke the MF operation in the context of the equivalent system model of (3), which is represented by

$$\mathbf{Z} = \acute{\mathbf{H}}^H \bar{\mathbf{Y}} \in \mathcal{C}^{Q\times 1}. \tag{6}$$

$$= \acute{\mathbf{H}}^H \bar{\mathbf{H}}\mathbf{K}_{q,l} + \acute{\mathbf{H}}^H \bar{\mathbf{V}} \tag{7}$$

noting that the complex-valued component of $\acute{\mathbf{H}}^H\bar{\mathbf{V}}$ also obeys the Gaussian distribution of $\mathcal{CN}(0, N_0)$. Here, let us approximate the conditional probability density function of $p(\mathbf{Z}|\mathbf{K}_{q,l})$ as

$$\frac{1}{(\pi N_0)^Q}\exp\left(-\frac{\|\mathbf{Z}-\|\bar{\mathbf{h}}_q\|\mathbf{K}_{q,l}\|^2}{N_0}\right) = \frac{1}{(\pi N_0)^Q}\exp\left(-\frac{\|\mathbf{Z}\|^2 - 2\Re\left[z_q^*\|\bar{\mathbf{h}}_q\|s_l\right] + \|\bar{\mathbf{h}}_q\|^2|s_l|^2}{N_0}\right). \tag{8}$$

Then, to calculate the extrinsic LLR outputs, the reduced-complexity MAP exhaustive search is applied to the MF signals $\mathbf{Z}$, which is formulated as (9) [10], [21], shown at the bottom of the page, where K_1^k and K_0^k represent the subspace of the legitimate equivalent signals K, satisfying $K_1^k \equiv \{\mathbf{K}_{q,l} \in K : b_k = 1\}$ and $K_0^k \equiv \{\mathbf{K}_{q,l} \in K : b_k = 0\}$. Furthermore, (9) is readily simplified by the max-log approximation [22], yielding

$$\begin{aligned} L_{\mathrm{e}}(b_k) &\simeq \max_{\mathbf{K}_{q,l}\in \mathrm{K}_1^k}\left[-\frac{\|\mathbf{Z}\|^2 - 2\Re\left[z_q^*\|\bar{\mathbf{h}}_q\|s_l\right] + \|\bar{\mathbf{h}}_q\|^2|s_l|^2}{N_0} + \sum_{j\neq k} b_j L_{\mathrm{apr}}(b_j)\right] \\ &\quad - \max_{\mathbf{K}_{q,l}\in \mathrm{K}_0^k}\left[-\frac{\|\mathbf{Z}\|^2 - 2\Re\left[z_q^*\|\bar{\mathbf{h}}_q\|s_l\right] + \|\bar{\mathbf{h}}_q\|^2|s_l|^2}{N_0} + \sum_{j\neq k} b_j L_{\mathrm{apr}}(b_j)\right] \\ &= \max_{\mathbf{K}_{q,l}\in \mathrm{K}_1^k}\left[-\frac{-2\Re\left[z_q^*\|\bar{\mathbf{h}}_q\|s_l\right] + \|\bar{\mathbf{h}}_q\|^2|s_l|^2}{N_0} + \sum_{j\neq k} b_j L_{\mathrm{apr}}(b_j)\right] \\ &\quad - \max_{\mathbf{K}_{q,l}\in \mathrm{K}_0^k}\left[-\frac{-2\Re\left[z_q^*\|\bar{\mathbf{h}}_q\|s_l\right] + \|\bar{\mathbf{h}}_q\|^2|s_l|^2}{N_0} + \sum_{j\neq k} b_j L_{\mathrm{apr}}(b_j)\right]. \end{aligned} \tag{10}$$

$$\begin{aligned} L_{\mathrm{e}}(b_k) &= \ln\frac{\sum_{\mathbf{K}_{q,l}\in \mathrm{K}_1^k} p(\mathbf{Z}|\mathbf{K}_{q,l})\cdot\exp\left[\sum_{j\neq k} b_j L_{\mathrm{apr}}(b_j)\right]}{\sum_{\mathbf{K}_{q,l}\in \mathrm{K}_0^k} p(\mathbf{Z}|\mathbf{K}_{q,l})\cdot\exp\left[\sum_{j\neq k} b_j L_{\mathrm{apr}}(b_j)\right]} \\ &\simeq \ln\frac{\sum_{\mathbf{K}_{q,l}\in \mathrm{K}_1^k}\exp\left[-\frac{\|\mathbf{Z}\|^2 - 2\Re\left[z_q^*\|\bar{\mathbf{h}}_q\|s_l\right] + \|\bar{\mathbf{h}}_q\|^2|s_l|^2}{N_0} + \sum_{j\neq k} b_j L_{\mathrm{apr}}(b_j)\right]}{\sum_{\mathbf{K}_{q,l}\in \mathrm{K}_0^k}\exp\left[-\frac{\|\mathbf{Z}\|^2 - 2\Re\left[z_q^*\|\bar{\mathbf{h}}_q\|s_l\right] + \|\bar{\mathbf{h}}_q\|^2|s_l|^2}{N_0} + \sum_{j\neq k} b_j L_{\mathrm{apr}}(b_j)\right]} \end{aligned} \tag{9}$$

The proposed detector is capable of approaching that of the max-log MAP detector, which will be explicitly shown in Section IV. In addition to reduced decoding complexity and improved achievable BER performance, a further merit of the proposed detector is that the proposed detector is capable of supporting arbitrary constellations, without any elaborate derivation, depending on the specific modulation constellations employed. Furthermore, the proposed detector is also capable of supporting not only $M \leq T$ but also $M > T$ scenarios. This allows us to exploit the benefits of the flexible rate-diversity tradeoff while substantially reducing the decoding complexity.

When considering a rapidly block-fading environment, the decoding complexity of the proposed detector of (10) per iteration was found to be

$$\text{Comp}_{(10)} = \frac{4MNTQ + 8NTQ + 4Q\mathcal{L} + 2Q}{\log_2(Q \cdot \mathcal{L})} \tag{11}$$

where we quantified the complexity in terms of the number of real-valued multiplications, according to [1]. For reference, the corresponding decoding complexity of the max-log MAP detector designed for the STSK scheme [1] may be expressed as

$$\text{Comp}_{\text{MAP}} = \frac{4MNTQ + 6NTQ\mathcal{L} + Q\mathcal{L}}{\log_2(Q \cdot \mathcal{L})}. \tag{12}$$

To avoid any digression, the decoding complexity of (11) and (12) is quantified in the Appendix.

III. Reduced-Complexity Soft-Decision Generalized Space-Time Shift Keying Detector

In this section, we develop a reduced-complexity SoD detector for the GSTSK scheme, which is derived based on the detector proposed in Section II. Then, we also present an optional approach based on the MCMC algorithm, which is capable of further reducing the complexity of the proposed GSTSK detector.

A. System Model of the GSTSK Scheme

We consider the three-stage-concatenated GSTSK scheme [10], where the STSK mapping block of Fig. 1 is replaced by the GSTSK mapping block. Here, we briefly introduce the GSTSK mapping principle, noting that the detailed explanations can be found, for example, in [2] and [10].

While the STSK activates only a single one out of the Q dispersion matrices $\mathbf{A}_q$, the GSTSK scheme activates P out of Q dispersion matrices, i.e., $\mathbf{A}^{(p)}$ $(p = 1, \ldots, P)$. Each of the activated matrices is multiplied by independently modulated PSK/QAM symbols $s^{(p)}$ $(p = 1, \ldots, P)$. To be more specific, during each block interval, $B = \log_2 f(Q, P) + P \log_2 \mathcal{L}$ bits are input to the GSTSK mapping block, where $f(Q, P) = 2^\iota$ satisfies the relationship of $2^\iota \leq \binom{Q}{P} < 2^{\iota+1}$ [10]. Then, the B bits are S/P converted to $B_1 = \log_2 f(Q, P)$ bits and $B_2 = P \log_2 \mathcal{L}$ bits. According to the B_1 input bits and the table specifying the mapping from the input bits to a dispersion-matrix subset, P dispersion matrices $\mathbf{A}^{(p)}$ $(p = 1, \ldots, P)$ are selected from $\mathbf{A}_q$ $(q = 1, \ldots, Q)$, whereas B_2 bits are mapped to independent P PSK/QAM symbols $s^{(p)}$ $(p = 1, \ldots, P)$. Finally, the GSTSK codeword $\mathbf{S}_b$ is generated as follows [10]:

$$\mathbf{S}_b = \sum_{p=1}^{P} s^{(p)} \mathbf{A}^{(p)} \tag{13}$$

where $b \in \{1, \ldots, 2^B\}$ represents the B input bits per block, and we have the power constraint of

$$\text{tr}\left[\mathbf{A}_q \mathbf{A}_q^H\right] = T/P \ (q = 1, \ldots, Q). \tag{14}$$

Similar to the STSK formulation of (3), we may arrive at the GSTSK receiver's signal model in the form of

$$\bar{\mathbf{Y}} = \bar{\mathbf{H}}\mathbf{K}_b + \bar{\mathbf{V}} \tag{15}$$

where we have $\mathbf{K}_b = [k_1, \ldots, k_Q]^T \in \mathcal{C}^{Q \times 1}$ and

$$k_q = \begin{cases} s^{(p)}, & q = g(b_1, p) \\ 0, & \text{else} \end{cases} \tag{16}$$

where $b_1 \in \{1, \ldots, B_1\}$ denotes the B_1 S/P converted bits. Furthermore, $g(b_1, p) \in \{1, \ldots, Q\}$ represents the index of the pth activated dispersion matrix, satisfying the relationship of $\mathbf{A}^{(p)} = \mathbf{A}_{g(b_1,p)}$. To elaborate a little further, it can be found from (15) and (16) that the equivalent signal vector $\mathbf{K}_b$ contains P nonzero signals; hence, in contrast to the IEI-free STSK scheme, the corresponding GSTSK receiver suffers from the effects of $(P-1)$ IEI contributions. For the sake of simplicity, we will employ the system description of "GSTSK(M, N, T, Q, P)" [10] in the rest of this paper. Note that the STSK(M, N, T, Q) scheme may be viewed as the special case of the GSTSK arrangement, i.e., STSK(M, N, T, Q) is equivalent to GSTSK$(M, N, T, Q, 1)$.

B. Proposed SoD GSTSK Detector

Similar to the STSK detector proposed in Section II, the modified MF operation of (5) and (6) is carried out to calculate the MF signal vector $\mathbf{Z} = [z_1, \ldots, z_Q]^T$ while assuming that channel matrix $\mathbf{H}$ and noise variance N_0 are perfectly acquired at the receiver. Then, we consider the approximate conditional probability density function of

$$\begin{aligned} &\frac{1}{(\pi N_0)^Q} \exp\left(-\frac{\|\mathbf{Z} - \mathbf{X}_b\|^2}{N_0}\right) \\ &\quad = \frac{1}{(\pi N_0)^Q} \exp\left(-\frac{\|\mathbf{Z}\|^2 - 2\Re[\mathbf{Z}^H \mathbf{X}_b] + \|\mathbf{X}_b\|^2}{N_0}\right) \end{aligned} \tag{17}$$

where we have $\mathbf{X}_b = [x_1^{(b)}, \ldots, x_Q^{(b)}]^T = \acute{\mathbf{H}}^H \bar{\mathbf{H}} \mathbf{K}_b \in \mathcal{C}^{Q \times 1}$. Since the qth element of $\mathbf{X}_b$ may be expressed as

$$x_q^{(b)} = \begin{cases} \left\|\bar{\mathbf{h}}_{g(b_1,p)}\right\| s^{(p)} + \sum_{p' \neq p} \frac{\bar{\mathbf{h}}_{g(b_1,p)}^H}{\left\|\bar{\mathbf{h}}_{g(b_1,p)}\right\|} \bar{\mathbf{h}}_{g(p')} s^{(p')}, & q = g(b_1, p) \\ \sum_{p=1}^{P} \frac{\bar{\mathbf{h}}_q^H}{\|\bar{\mathbf{h}}_q\|} \bar{\mathbf{h}}_{g(b_1,p)} s^{(p)}, & \text{else.} \end{cases} \tag{18}$$

Equation (17) may be further simplified to

$$\frac{1}{(\pi N_0)^Q}\exp\left(-\frac{\left[\|\mathbf{Z}\|^2-\sum_{q=1}^{Q}\left\{2\Re\left[z_q^* x_q^{(b)}\right]-\left|x_q^{(b)}\right|^2\right\}\right]}{N_0}\right).$$

Finally, similar to (9), the extrinsic LLR output of the proposed GSTSK detector is given by (19), shown at the bottom of the page, and its max-log approximation is written by

$$\begin{aligned}L_{\mathrm{e}}(b_k)=&\max_{\mathbf{K}_b\in\mathrm{K}_1^k}\left[-\frac{\|\mathbf{Z}\|^2-\sum_{q=1}^{Q}\left\{2\Re\left[z_q^* x_q^{(b)}\right]-\left|x_q^{(b)}\right|^2\right\}}{N_0}+\sum_{j\neq k}b_j L_{\mathrm{apr}}(b_j)\right]\\&-\max_{\mathbf{K}_b\in\mathrm{K}_0^k}\left[-\frac{\|\mathbf{Z}\|^2-\sum_{q=1}^{Q}\left\{2\Re\left[z_q^* x_q^{(b)}\right]-\left|x_q^{(b)}\right|^2\right\}}{N_0}+\sum_{j\neq k}b_j L_{\mathrm{apr}}(b_j)\right]\\=&\max_{\mathbf{K}_b\in\mathrm{K}_1^k}\left[\frac{\sum_{q=1}^{Q}\left\{2\Re\left[z_q^* x_q^{(b)}\right]-\left|x_q^{(b)}\right|^2\right\}}{N_0}+\sum_{j\neq k}b_j L_{\mathrm{apr}}(b_j)\right]\\&-\max_{\mathbf{K}_b\in\mathrm{K}_0^k}\left[\frac{\sum_{q=1}^{Q}\left\{2\Re\left[z_q^* x_q^{(b)}\right]-\left|x_q^{(b)}\right|^2\right\}}{N_0}+\sum_{j\neq k}b_j L_{\mathrm{apr}}(b_j)\right].\end{aligned}\tag{20}$$

The decoding complexity per bit of the proposed SoD-aided GSTSK detector of (20) may be represented by

$$\begin{aligned}\mathrm{Comp}_{(20)}=&\frac{1}{B}\left\{4MNTQ+8NTQ+Q(Q-1)\right.\\&\left.\times(2NT+4\mathcal{L})+1)+2Q+(4Q+1)2^B\right\}\end{aligned}\tag{21}$$

whereas that of the max-log MAP detector is given by

$$\mathrm{Comp}_{\mathrm{MAP}}=\frac{4MNTQ+NT(4P+2)2^B+2^B}{B}.\tag{22}$$

Furthermore, we emphasized that, although exhaustive symbol search is needed for the proposed detectors of (19) and (20), the decoding complexity is reduced from their MAP-detector based counterpart, which is an explicit benefit of the MF operation. The performance difference between (21) and (22) will be evaluated later in Section IV.

C. Incorporation of MCMC Into the Proposed SoD GSTSK Detector

In this section, we incorporate the MCMC concept into our MF-based detector. This allows us to reduce the search space of (20) by efficiently sampling only the most likely signals, rather than considering the 2^B legitimate signals of the MAP detector.

More specifically, the Gibbs-Sampler is employed in this paper for sampling the corresponding signals [16], [20]. In the Gibbs-Sampler [16], N_{P} independent chains are considered, where each chain contains N_{MC} correlated signal sampling. Considering that the resultant $N_{\mathrm{P}}\cdot N_{\mathrm{MC}}$ signals may contain overlapping signals, we finally have $\gamma<N_{\mathrm{P}}\cdot N_{\mathrm{MC}}$ different signals $\mathbf{X}^{(i)}=[x_1^{(i)},\ldots,x_Q^{(i)}]^T$ $(i=1,\ldots,\gamma)$ at the output of the Gibbs-Sampler, which are then tested against the MF-based max-log MAP criterion of (20).

Here, the complexity of the proposed MF-MCMC-aided GSTSK detector is given by

$$\begin{aligned}\mathrm{Comp}_{\mathrm{MCMC}}=&\frac{1}{B}\left\{4MNTQ+8NTQ+Q(Q-1)\right.\\&\left.\times(2NT+4\mathcal{L})+1+2Q+(4Q+1)\gamma\right\}.\end{aligned}\tag{23}$$

We note that, since, in the MCMC algorithms, the number of samples N_{MC} is typically lower than the number of legitimate signals 2^B, the associated complexity of (23) becomes lower than that of the original MF-based GSTSK detector of (21).

To expound a little further, the decoding complexity of our MF-based detector proposed in Section III-B remains constant, regardless of the signal-to-noise ratio (SNR) and of the *a priori* LLRs, whereas that of the MCMC- and MF-aided detector proposed in this section is affected by these two parameters. Hence, when the SNR and the *a priori* LLRs are high, the Gibbs-Sampler rapidly converges, and therefore, the resultant number of sampled signals γ becomes low.

$$L_{\mathrm{e}}(b_k)=\ln\frac{\sum_{\mathbf{K}_b\in\mathrm{K}_1^k}\exp\left[-\frac{\|\mathbf{Z}\|^2-\sum_{q=1}^{Q}\left\{2\Re\left[z_q^* x_q^{(b)}\right]-\left|x_q^{(b)}\right|^2\right\}}{N_0}+\sum_{j\neq k}b_j L_{\mathrm{apr}}(b_j)\right]}{\sum_{\mathbf{K}_b\in\mathrm{K}_0^k}\exp\left[-\frac{\|\mathbf{Z}\|^2-\sum_{q=1}^{Q}\left\{2\Re\left[z_q^* x_q^{(b)}\right]-\left|x_q^{(b)}\right|^2\right\}}{N_0}+\sum_{j\neq k}b_j L_{\mathrm{apr}}(b_j)\right]}\tag{19}$$

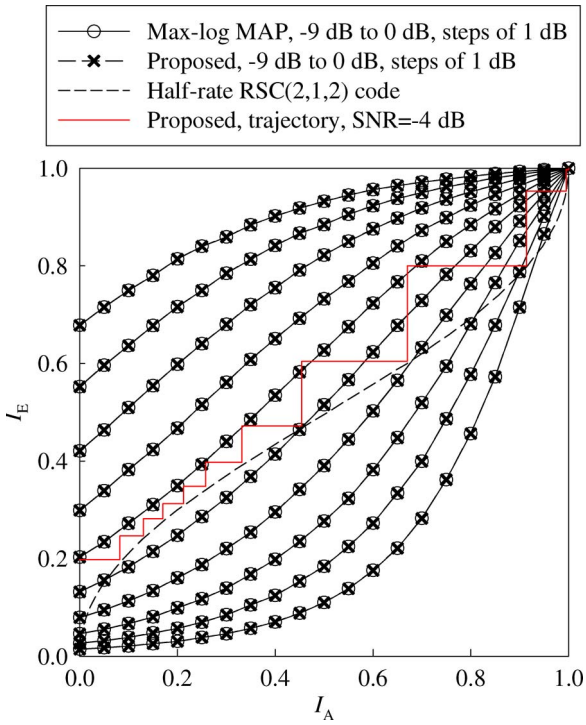

Fig. 2. EXIT-chart comparison of the proposed detector and the max-log MAP detector for the three-stage RSC- and URC-coded STSK(4, 4, 2, 4) scheme employing QPSK. Note that the STSK(4, 4, 2, 4) mapping block corresponds to the GSTSK(4, 4, 2, 4, 1) mapping block. In addition, the EXIT curve of the half-rate RSC(2, 1, 2) code and the EXIT trajectory of the proposed detector at SNR $= -4$ dB were plotted.

IV. Simulation Results

In this section, we provide our simulation results for the sake of characterizing both the achievable performance and the decoding complexity of the proposed detector. Here, we considered the three-stage-concatenated[3] RSC- and URC-coded GSTSK scheme of Fig. 1. The number of transmit and receive antennas was given by $M = N = 4$. A half-rate memory-two RSC(2, 1, 2) scheme having the octal generator polynomials of $(G_r, G) = (3, 2)_8$ was employed for the channel encoder, whereas the length of the interleavers Π_1 and Π_2 was set to 200 000 bits. At the receiver, the number of inner and outer iterations was chosen to be $I_{\rm in} = 2$ and $I_{\rm out} = 20$.[4] Furthermore, we assumed rapid Rayleigh block-fading channels. To optimize the dispersion-matrix set, the Discrete-input Continuous-output Memoryless Channel (DCMC) capacity maximization criterion [1] was employed, which enables the direct improvement of the GSTSK scheme's maximum achievable rate.

First, Fig. 2 shows the EXtrinsic Information Transfer (EXIT) chart (a tutorial was provided for example in [22]) of the RSC- and URC-coded STSK(4, 4, 2, 4) scheme using quadratic phase-shift keying (QPSK) modulation, where we considered both the max-log MAP detector [1] and the detector proposed in Section II-B. Here, the SNR was varied from -9 to 0 dB in steps of 1 dB. Furthermore, the Monte-Carlo-simulation-based EXIT trajectory of the proposed detector recorded at SNR $= -4$ dB and the EXIT curve of the RSC(2, 1, 2) code were also plotted. Observe in Fig. 2 that both the detectors exhibited similar curves, implying that the proposed SoD STSK detector is capable of approaching the near-capacity performance[5] attained by the max-log MAP detector.

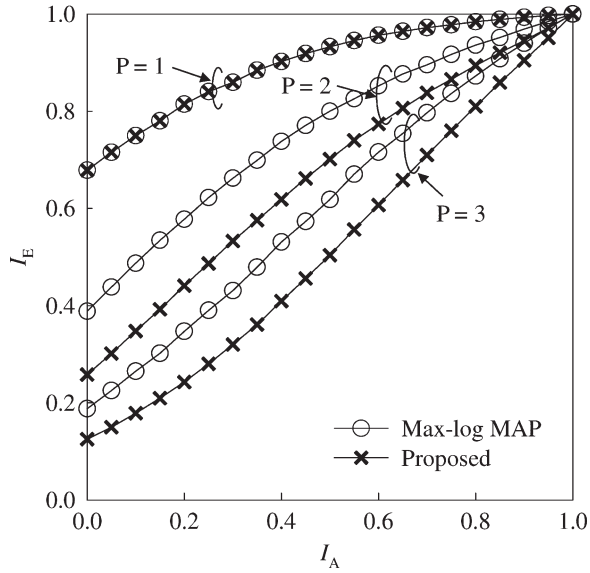

Fig. 3. EXIT-chart comparison of the proposed detector and the max-log MAP detector for the three-stage RSC- and URC-coded GSTSK(4, 4, 2, 4, P) scheme employing QPSK for SNR $= 0$ dB.

Next, in Fig. 3, we compared the three different GSTSK(4, 4, 2, 4, P) schemes associated with $P = 1$ to 3 using QPSK modulation at SNR $= 0$ dB. Note that the $P = 1$ GSTSK scenario of Fig. 3 corresponds to the STSK scheme characterized in Fig. 2. It was found from Fig. 3 that, while the proposed STSK detector of Section II-B did not exhibit any performance loss in comparison to the max-log MAP detector for the $P = 1$ STSK scenario, the GSTSK detector of Section III-B imposes a slight performance erosion between the two detectors for $P = 2$ and 3.

To provide further insights, Fig. 4 shows the maximum achievable rate of these three GSTSK arrangements employing both the proposed detector and the max-log MAP detector. Here, the maximum achievable rates were calculated by evaluating the area under the corresponding detector's EXIT curve, as argued in [21] and [24]. We also plotted the DCMC capacity [21] as a bound, which takes into account the modulation-specific constraints of the GSTSK signaling. As predicted, it can be seen from Fig. 4 that, for $P = 1$, our STSK detector's curve coincided with that of the max-log MAP benchmarker, representing near-optimal performance. On the other hand, it was found that, for $P \geq 2$, our GSTSK detector exhibited a slight performance loss of 1–2 dB, in comparison to that

[3]Again, the additional benefits of using a three-stage rather than two-stage architecture were detailed in [21] and [22].

[4]According to [21] and our related extensive simulations, an increase in the number of inner iterations $I_{\rm in}$ after $I_{\rm in} = 2$ was found not to provide any substantial performance improvement. Thus, the number of inner iterations was set to $I_{\rm in} = 2$ in our simulations.

[5]An important property of EXIT charts is that, if the decoding trajectory reaches the (1, 1) point of perfect iterative decoding convergence, an infinitesimally low BER is attainable. This is because, in the presence of perfect *a priori* information, perfect *a posteriori* information is generated.

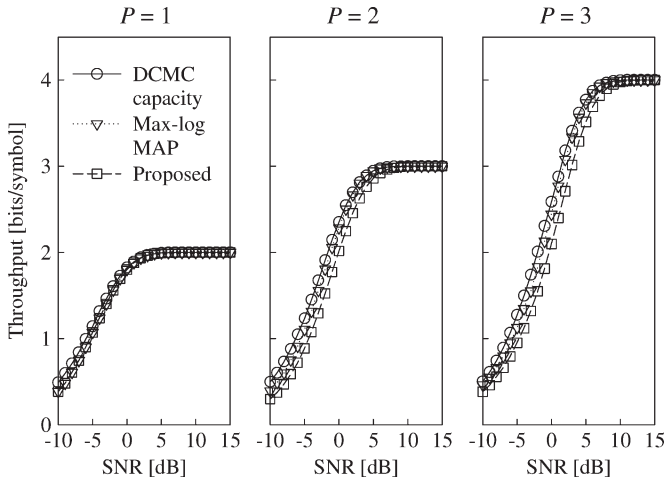

Fig. 4. Comparisons of the maximum achievable rate between the proposed detector and the max-log MAP detector for the QPSK-modulated GSTSK(4, 4, 2, 4, P) scheme, where the value of P was varied from $P = 1$ to 3. Here, the corresponding DCMC capacity curves were also plotted.

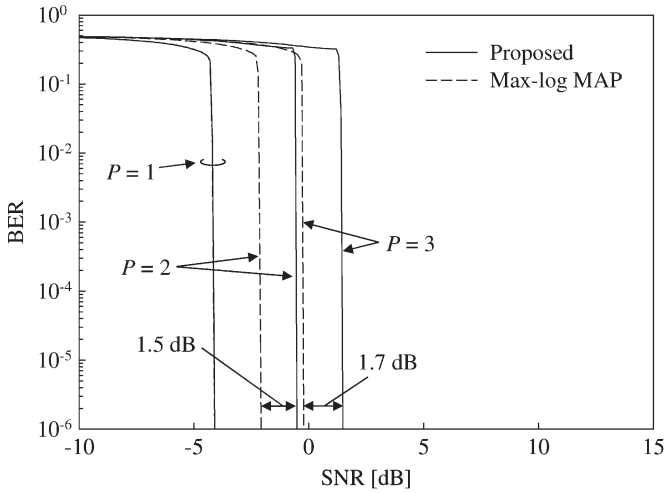

Fig. 5. Achievable BER performance of the three-stage-concatenated RSC(2, 1, 2)- and URC-coded GSTSK(4, 4, 2, 4, P) schemes assisted by QPSK modulation, employing the proposed detector and the max-log MAP detector, where the value of P was varied from $P = 1$ to 3. The normalized throughput is given by $R = 1$, 1.5, and 2 bit/symbol for $P = 1$, 2, and 3, respectively.

of the max-log MAP detector. Moreover, Fig. 5 shows the corresponding BER performance of the GSTSK scheme, which exactly matched the performance predicted by the EXIT-chart analysis.

Next, we investigated our MCMC-MF-aided GSTSK detector of Section III-C. Fig. 6 shows the number of signals sampled by the Gibbs-Sampler in the QPSK-modulated GSTSK(4, 4, 2, 4, 3) scheme. More specifically, in Fig. 6(a), the SNR was varied from 0 to 3 dB, and the Gibbs-Sampler's parameters were set to $N_{\rm MC} = N_{\rm P} = 8$; in Fig. 6(b), we considered $N_{\rm MC} = N_{\rm P} = 7$, 8, 9, and 10 at SNR $= 2$ dB. Observe in both Fig. 6(a) and (b) that, upon increasing the SNR and the *a priori* LLRs, the number of sampled signals is reduced. In this specific scenario, the number of sampled signals tended to be a half the legitimate signals $2^B = 2^8 = 256$; hence, the signal-search space was substantially reduced.

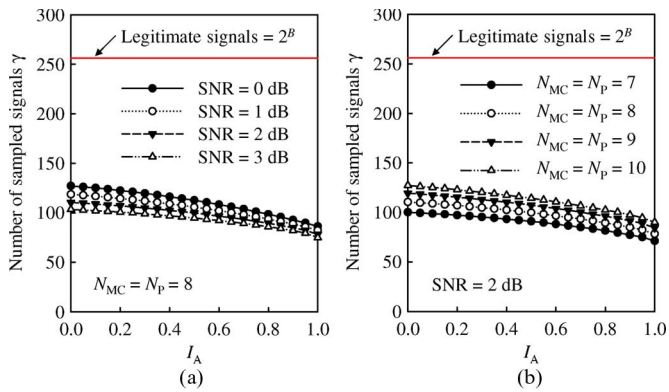

Fig. 6. Number of signals sampled by the Gibbs-Sampler in the QPSK-modulated GSTSK(4, 4, 2, 4, 3) scheme, having the number of legitimate signals $2^B = 2^8 = 256$. (a) SNR $= 0$, 1, 2, and 3 dB with fixed parameters of $N_{\rm MC} = N_{\rm P} = 8$ (b) $N_{\rm MC} = N_{\rm P} = 7$, 8, 9, and 10 for SNR $= 2$ dB.

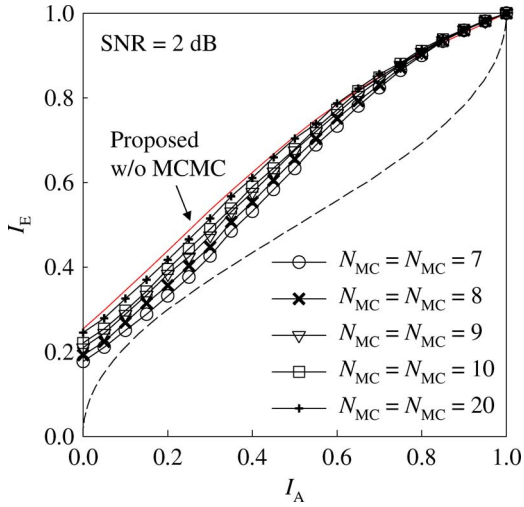

Fig. 7. EXIT chart of the proposed detector combined with the Gibbs-Sampler for the three-stage RSC- and URC-coded GSTSK(4, 4, 2, 4, P) scheme employing QPSK for SNR $= 2$ dB.

Additionally, Fig. 7 compared the EXIT curves of the proposed MCMC-MF-aided GSTSK detector, where the Gibbs-Sampler's parameters were given by $N_{\rm MC} = N_{\rm P} = 7$, 8, 9, 10, and 20 for SNR $= 2$ dB. Observe in Fig. 7 that, as predicted, the higher the values of $N_{\rm MC}$ and $N_{\rm P}$, the closer the associated EXIT curve to that of the MF-based detector.

Finally, in Fig. 8, we compared the decoding complexity of the proposed MF-based and MCMC-MF-aided detectors and that of the max-log MAP detector, where the MF-based detector is capable of reducing the max-log MAP detector's complexity by 35%, 60%, and 81% for the $P = 1$, 2, and 3 scenarios, respectively. Explicitly, upon increasing P, i.e., the throughput, the attainable complexity reduction is increased. Furthermore, as shown in Fig. 8, the MCMC algorithm further reduced its complexity to 51% of the MF-based detector's complexity, which is about 9.7% of the max-log MAP detector for $P = 3$.

V. Conclusion

In this paper, we have first proposed a novel reduced-complexity SoD-assisted STSK detector that is capable of

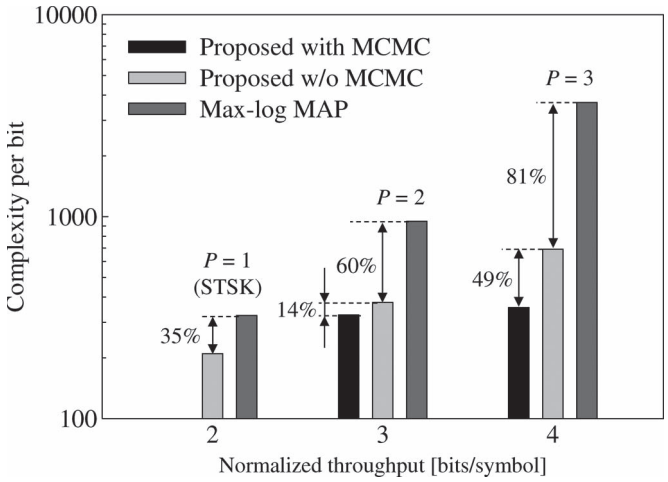

Fig. 8. Relationship between the normalized throughput of the GSTSK-mapping block and the decoding complexity for the QPSK-modulated GSTSK(4, 4, 2, 4, P) scheme, where the number of activated dispersion matrices was varied from $P = 1$ to 3. The parameters employed for the Gibbs-Sampler were set to $N_{\rm MC} = N_{\rm P} = 8$. Here, the decoding complexity was evaluated in terms of the number of real-valued multiplications.

approaching the optimal MAP performance. Moreover, we have extended this detector to support our iteratively detected GSTSK scheme. A further contribution is that we intrinsically amalgamated the MCMC algorithm with our GSTSK detector to reduce the decoding complexity imposed. As a result, the proposed detector is applicable to diverse channel-coded MIMO systems, which are subsumed by the GSTSK scheme. This allows us to benefit from a near-capacity MIMO performance while substantially reducing the decoding complexity of the MAP detector.

APPENDIX

Here, the decoding complexity of the proposed SoD STSK detector of (10) is evaluated in a similar manner to [15]. Assuming that the receiver stores the power of each constellation point $|s_l|^2$ $(l = 1, \ldots, \mathcal{L})$ and channels $\mathbf{H}$ are successfully estimated, the complexity cost of the equivalent channels $\bar{\mathbf{H}} = (\mathbf{I}_T \otimes \mathbf{H})\chi$ is given by

$$\text{comp}\left[(\mathbf{I}_T \otimes \mathbf{H})\chi\right] = 4MNTQ \tag{24}$$

where "comp[·]" represents the number of real-valued multiplications, which is required for calculating "·." Then, the norm of each column of $\bar{\mathbf{H}}$, i.e., $\|\bar{\mathbf{h}}_q\|$ $(q = 1, \ldots, Q)$, is computed at a complexity of

$$\text{comp}\left[\|\bar{\mathbf{h}}_q\| \ (q = 1, \ldots, Q)\right] = 2NTQ. \tag{25}$$

Then, the calculation of $\acute{\mathbf{H}} = [\bar{\mathbf{h}}_1/\|\bar{\mathbf{h}}_1\| \cdots \bar{\mathbf{h}}_Q/\|\bar{\mathbf{h}}_Q\|]$ in (5) imposes a complexity of

$$\text{comp}[\acute{\mathbf{H}}] = 2NTQ. \tag{26}$$

Furthermore, the MF operation of (6) imposes a complexity of

$$\text{comp}[\acute{\mathbf{H}}^H \bar{\mathbf{Y}}] = 4NTQ \tag{27}$$

whereas the rest of the calculations imposed by (10) is given as follows:

$$\text{comp}\left[\frac{\|\bar{\mathbf{h}}_q\|}{N_0}(q = 1, \ldots, Q)\right] = Q \tag{28}$$

$$\text{comp}\left[\frac{\|\bar{\mathbf{h}}_q\|^2}{N_0}(q = 1, \ldots, Q)\right] = Q \tag{29}$$

$$\text{comp}\left[\frac{\|\bar{\mathbf{h}}_q\|^2}{N_0}\right] = Q \tag{30}$$

$$\text{comp}\left[\frac{\|\bar{\mathbf{h}}_q\|^2|s_l|^2}{N_0}\ (q = 1, \ldots, Q, l = 1, \ldots, \mathcal{L})\right] = Q\mathcal{L} \tag{31}$$

$$\text{comp}\left[\frac{\Re\left[z_q^*\|\bar{\mathbf{h}}_q\|s_l\right]}{N_0}\ (q = 1, \ldots, Q, l = 1, \ldots, \mathcal{L})\right] = 3Q\mathcal{L}. \tag{32}$$

Finally, it was found from (24)–(32) that the total calculation cost may be approximated by (11).

In the same manner, we also evaluate the decoding complexity of the max-log MAP STSK detector, which is represented by [1]

$$L_{\rm e}(b_k) \simeq \max_{\mathbf{K}_{q,l} \in \mathrm{K}_1^k}\left[-\frac{\|\bar{\mathbf{Y}} - \bar{\mathbf{H}}\mathbf{K}_{q,l}\|^2}{N_0} + \sum_{j \neq k} b_j L_{\rm apr}(b_j)\right] - \max_{\mathbf{K}_{q,l} \in \mathrm{K}_0^k}\left[-\frac{\|\bar{\mathbf{Y}} - \bar{\mathbf{H}}\mathbf{K}_{q,l}\|^2}{N_0} + \sum_{j \neq k} b_j L_{\rm apr}(b_j)\right].$$

Considering that we have

$$\text{comp}\left[\bar{\mathbf{H}}\mathbf{K}_{q,l}\ (q = 1, \ldots, Q, l = 1, \ldots, \mathcal{L})\right] = 4NTQ\mathcal{L} \tag{33}$$

$$\text{comp}\left[\|\bar{\mathbf{Y}} - \bar{\mathbf{H}}\mathbf{K}_{q,l}\|^2\ (q = 1, \ldots, Q, l = 1, \ldots, \mathcal{L})\right] = 2NTQ\mathcal{L} \tag{34}$$

$$\text{comp}\left[\frac{\|\bar{\mathbf{Y}} - \bar{\mathbf{H}}\mathbf{K}_{q,l}\|^2}{N_0}\ (q = 1, \ldots, Q, l = 1, \ldots, \mathcal{L})\right] = Q\mathcal{L} \tag{35}$$

the resultant total decoding complexity of (12) can be obtained from (24) and (33)–(35).

REFERENCES

[1] S. Sugiura, S. Chen, and L. Hanzo, "Coherent and differential space-time shift keying: A dispersion matrix approach," *IEEE Trans. Commun.*, vol. 58, no. 11, pp. 3219–3230, Nov. 2010.

[2] S. Sugiura, S. Chen, and L. Hanzo, "A universal space-time architecture for multiple-antenna aided systems," *IEEE Commun. Surveys Tuts.*, vol. 14, no. 2, pp. 401–420, Second Quarter, 2012.

[3] J. Jeganathan, A. Ghrayeb, L. Szczecinski, and A. Ceron, "Space shift keying modulation for MIMO channels," *IEEE Trans. Wireless Commun.*, vol. 8, no. 7, pp. 3692–3703, Jul. 2009.

[4] M. Di Renzo and H. Haas, "Improving the performance of space shift keying (SSK) modulation via opportunistic power allocation," *IEEE Commun. Lett.*, vol. 14, no. 6, pp. 500–502, Jun. 2010.

[5] M. Di Renzo and H. Haas, "A general framework for performance analysis of space shift keying (SSK) modulation for MISO correlated Nakagami-m fading channels," *IEEE Trans. Commun.*, vol. 58, no. 9, pp. 2590–2603, Sep. 2010.

[6] R. Y. Mesleh, H. Haas, S. Sinanovic, C. Ahn, and S. Yun, "Spatial modulation," *IEEE Trans. Veh. Technol.*, vol. 57, no. 4, pp. 2228–2241, Jul. 2008.

[7] J. Jeganathan, A. Ghrayeb, and L. Szczecinski, "Spatial modulation: Optimal detection and performance analysis," *IEEE Commun. Lett.*, vol. 12, no. 8, pp. 545–547, Aug. 2008.
[8] R. Y. Mesleh, M. Di Renzo, H. Haas, and P. M. Grant, "Trellis coded spatial modulation," *IEEE Trans. Wireless Commun.*, vol. 9, no. 7, pp. 2349–2361, Jul. 2010.
[9] E. Basar, U. Aygolu, E. Panayirci, and H. Poor, "New trellis code design for spatial modulation," *IEEE Trans. Wireless Commun.*, vol. 10, no. 8, pp. 2670–2680, Aug. 2011.
[10] S. Sugiura, S. Chen, and L. Hanzo, "Generalized space-time shift keying designed for flexible diversity-, multiplexing- and complexity-tradeoffs," *IEEE Trans. Wireless Commun.*, vol. 10, no. 4, pp. 1144–1153, Apr. 2011.
[11] B. Hassibi and B. Hochwald, "High-rate codes that are linear in space and time," *IEEE Trans. Inf. Theory*, vol. 48, no. 7, pp. 1804–1824, Jul. 2002.
[12] J. Jeganathan, A. Ghrayeb, and L. Szczecinski, "Generalized space shift keying modulation for MIMO channels," in *Proc. IEEE 19th Int. Symp. PIMRC*, Cannes, France, Sep. 15–18, 2008, pp. 1–5.
[13] A. Younis, N. Serafimovski, R. Mesleh, and H. Haas, "Generalised spatial modulation," in *Proc. 44th Asilomar Conf. Signals, Syst. Comput.*, Pacific Grove, CA, Nov. 7–10, 2010, pp. 1498–1502.
[14] A. Younis, R. Mesleh, H. Haas, and P. Grant, "Reduced complexity sphere decoder for spatial modulation detection receivers," in *Proc. IEEE GLOBECOM*, Miami, FL, Dec. 6–10, 2010, pp. 1–5.
[15] S. Sugiura, C. Xu, S. X. Ng, and L. Hanzo, "Reduced-complexity coherent versus non-coherent QAM-aided space-time shift keying," *IEEE Trans. Commun.*, vol. 59, no. 11, pp. 3090–3101, Nov. 2011.
[16] S. Sugiura, S. Chen, and L. Hanzo, "MIMO-aided near-capacity turbo transceivers: Taxonomy and performance versus complexity," *IEEE Commun. Surveys Tuts.*, vol. 14, no. 2, pp. 421–442, Second Quarter, 2012.
[17] C. Berrou, A. Glavieux, and P. Thitimajshima, "Near shannon limit error-correcting coding and decoding: Turbo-codes," in *Proc. IEEE ICC*, Geneva, Switzerland, May 1993, vol. 2, pp. 1064–1070.
[18] W. Ryan and S. Lin, *Channel Codes: Classical and Modern*. Cambridge, U.K.: Cambridge Univ. Press, 2009.
[19] C. Xu, S. Sugiura, S. X. Ng, and L. Hanzo, "Reduced-complexity soft-decision aided space-time shift keying," *IEEE Signal Process. Lett.*, vol. 18, no. 10, pp. 547–550, Oct. 2011.
[20] B. Farhang-Boroujeny, H. Zhu, and Z. Shi, "Markov chain Monte Carlo algorithms for CDMA and MIMO communication systems," *IEEE Trans. Signal Process.*, vol. 54, no. 5, pp. 1896–1909, May 2006.
[21] L. Hanzo, O. Alamri, M. El-Hajjar, and N. Wu, *Near-Capacity Multi-Functional MIMO Systems: Sphere-Packing, Iterative Detection and Cooperation*. Hoboken, NJ: Wiley, 2009.
[22] L. Hanzo, T. Liew, B. Yeap, R. Y. S. Tee, and S. X. Ng, *Turbo Coding, Turbo Equalisation, and Space-Time Coding for Transmission Over Fading Channels*. Hoboken, NJ: Wiley, 2011.
[23] D. Divsalar, S. Dolinar, and F. Pollara, "Serial concatenated trellis coded modulation with rate-1 inner code," in *Proc. IEEE Global Telecommun. Conf.*, San Francisco, CA, Nov./Dec. 2000, vol. 2, pp. 777–782.
[24] S. ten Brink, G. Kramer, and A. Ashikhmin, "Design of low-density parity-check codes for modulation and detection," *IEEE Trans. Commun.*, vol. 52, no. 4, pp. 670–678, Apr. 2004.

Shinya Sugiura (M'06–SM'12) received the B.S. and M.S. degrees in aeronautics and astronautics from Kyoto University, Kyoto, Japan, in 2002 and 2004, respectively, and the Ph.D. degree in mobile communications from the University of Southampton, Southampton, U.K., in 2010.

Since 2004, he has been with Toyota Central R&D Laboratories, Inc., Nagakute, Japan, where his research has covered a range of areas in wireless communications, networking, signal processing, and antenna design. He authored or coauthored more than 45 refereed research publications, including 20 IEEE journal and magazine papers.

Dr. Suguira has received a number of distinctions, including the 2011 IEEE Commucations Society Asia-Pacific Outstanding Young Researcher Award, the 2011 Ericsson Young Scientist Award, and the 2008 IEEE Antennas and Propagation Society Japan Chapter Young Engineer Award.

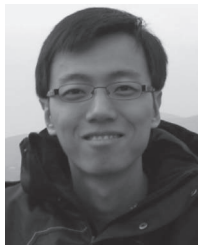

Chao Xu (S'09) received the B.Eng. degree in telecommunications engineering with management from Beijing University of Posts and Telecommunications, Beijing, China, and the B.Sc. (Eng) (with first-class honors) in telecommunications engineering with management from Queen Mary University of London, London, U.K., through a Sino-U.K. joint degree program, in 2008 and the M.Sc. degree (with distinction) in radio-frequency communication systems from the University of Southampton, Southampton, U.K., in 2009. He is currently working toward the Ph.D. degree with the Communications Research Group, School of Electronics and Computer Science, University of Southampton.

His research interests include reduced-complexity multiple-input–multiple-output design, noncoherent space-time modulation detection, and EXtrinsic Information Transfer (EXIT)-chart-aided turbo detection, as well as cooperative communications.

Mr. Xu received the IEEE Communications Society U.K. and RI Chapter Best M.Sc. Student in Broadband and Mobile Communication Networks Award.

Soon Xin Ng (S'99–M'03–SM'08) received the B.Eng. degree (First Class) in electronics engineering and the Ph.D. degree in wireless communications from the University of Southampton, Southampton, U.K., in 1999 and 2002, respectively.

From 2003 to 2006, he was a Postdoctoral Research Fellow, working on collaborative European research projects such as SCOUT, NEWCOM, and PHOENIX. Since August 2006, he has been a member of the academic staff with the School of Electronics and Computer Science, University of Southampton. He is involved in the OPTIMIX European project, as well as the IU-ATC and UC4G projects. He has authored more than 120 papers and coauthored two John Wiley/IEEE Press books in this field. His research interests include adaptive-coded modulation, coded modulation, channel coding, space-time coding, joint source and channel coding, iterative detection, orthogonal frequency-division multiplexing, multiple-input multiple-output, cooperative communications, and distributed coding.

Dr. Ng is a Fellow of the Higher Education Academy of the U.K.

Lajos Hanzo (M'91–SM'92–F'04) received the Master's, the Ph.D., and Honorary Doctorate "Doctor Honaris Causa" degrees from the Technical University of Budapest, Budapest, Hungary, in 1976, 1983, and 2009, respectively.

During his 34-year career in telecommunications, he has held various research and academic posts in Hungary, Germany, and the U.K. Since 1986, he has been with the School of Electronics and Computer Science, University of Southampton, Southampton, U.K., where he holds the chair in telecommunications. He is also a Chaired Professor with Tsinghua University, Beijing, China. He has coauthored 20 John Wiley-IEEE Press books on mobile radio communications, totaling in excess of 10 000 pages; authored more than 1200 research papers and book chapters, on IEEE Xplore; acted as Technical Program Committee Chair of IEEE conferences; presented keynote lectures; and received a number of distinctions. He is currently directing an academic research team, working on a range of research projects in the field of wireless multimedia communications sponsored by industry, the Engineering and Physical Sciences Research Council U.K., the European IST Programme, and the Mobile Virtual Centre of Excellence, U.K. He is an enthusiastic supporter of industrial and academic liaison, and he offers a range of industrial courses.

Dr. Hanzo is a Fellow of the Royal Academy of Engineering and the Institution of Engineering and Technology. He is an IEEE Distinguished Lecturer and a Governor of both the IEEE Communications and Vehicular Technology Societies and the Editor-in-Chief of the IEEE Press.